Science and Technology Indonesia
e-ISSN:2580-4391 *p*-ISSN:2580-4405
Vol. 9, No. 1, January 2024

Research Paper

The Utilization of Candlenut Shell-Based Activated Charcoal as the Electrode of Capacitive Deionization (CDI) for Seawater Desalination

Muhammad Anas[1], Mardiana Napirah[1*], Wa Ode Sitti Ilmawati[2], Husein[1], Amiruddin Takda[1], Like Herawati[1], Ima[1], Karmila Sari[1]

[1]*Department of Physics Education, Faculty of Teacher Training and Education, Universitas Halu Oleo, Jl. H.E.A. Mokodompit No. 1, Kendari, 93232, Indonesia*
[2]*Department of Physics, Faculty of Mathematics and Natural Sciences, Universitas Halu Oleo, Jl. H.E.A. Mokodompit No. 1, Kendari, 93232, Indonesia*
*__Corresponding author__: mardiana.napirah@uho.ac.id

Abstract
Activated carbon or activated charcoal is one of the best materials that can be used as a constituent of CDI electrodes, not only because of its various advantageous properties but also because it can be sourced abundantly from plant waste. This research aims to determine the effect of the thickness of the candlenut shell activated charcoal electrode and the particle size of the activated carbon used on the capacitive deionization (CDI) performance in seawater desalination. Candlenut shell-based activated charcoal is obtained in three stages, namely preparation, carbonization, and activation. The carbonization stage was done by using a pyrolysis reactor at a temperature of 400°C for 8 hours. The activation was done with the activator of H_3PO_4 67%. The variation of thickness was 6 mm, 8 mm, 10 mm, and 15 mm while the variation of particle size was 60 mesh, 80 mesh, 100 mesh, and 200 mesh. The results showed that the higher capacitance was obtained with the thinner electrodes, where the best value was the thinnest electrode, 6 mm, which produced the highest capacitance, 122.96 nF. For the desalination of seawater, it is shown that the finest particle/smallest particle size will result in the best desalination performance, where 200 mesh particle size will result in the decrease of salinity from 34% to 4%. That is 88.23% decrease in salinity. Therefore, the using of candlenut shell-based activated carbon as the electrode in CDI is proven to be able to obtain good performance in seawater desalination.

Keywords
Capacitive Deionization, Candlenut Shell-Based Activated Carbon, Electrode, Seawater Desalination

Received: 21 December 2022, Accepted: 22 November 2023
https://doi.org/10.26554/sti.2024.9.1.86-93

1. INTRODUCTION

Water is an essential requirement utilized across various facets of human existence. Clean water is indispensable for routine activities, such as drinking, culinary preparations, personal hygiene, laundering, and sanitation. Unfortunately, water insufficiency constitutes a prevalent issue encountered in certain geographical areas. This predicament persists even in proximity to certain water sources due to clean water shortages. Scarcity is a serious global challenge in our era. Research conducted by He et al. indicates a projected increase in the urban population facing water scarcity issues from 933 million people in 2016 to 1.693 – 2.373 billion by the year 2050. An increase from one-third of the global urban population in 2016 to almost half of the global urban population by the year 2050 (He et al., 2021). Despite 70% of the Earth's surface being covered by water, only 2.7% of it constitutes fresh water. Even just 0.3% of fresh water is consumable by humans. Most of the earth's water bodies that cover the surface are seawater, which is unfit for human consumption due to its high salinity, approximately 3% (Gong et al., 2019; Zapata-Sierra et al., 2021).

Seawater desalination is considered a promising solution to the water scarcity crisis in the world. It is done by removing salt as well as other mineral components from seawater. There are many types of desalination process, but among all of these processes, the desalination technologies used in industrial scale are Reverse Osmosis (RO), Multi Effect Distillation (MED), and Multi Stage Flash Distillation (MSFD) (Naseer et al., 2022). Despite its significant advantages in converting seawater into clean water, desalination technology is still perceived as financially burdensome (Lin et al., 2021; Mohammadi et al., 2020). To obtain low-cost desalination technology, many researches have been conducted since 2000. Among all of the desalination technologies being developed, capacitive deionization is one of the eminent topic (Naseer et al., 2022).

Capacitive deionization (CDI) has garnered significant interest in the last decade due to its straightforward ion removal from water, along with its environmental-friendliness, affordability, minimal energy usage, and easy electrode regeneration

(Xing et al., 2020). The fundamental concept behind a CDI process is as follows. When a voltage difference (typically up to 1.2 V) is applied to the CDI cell, which consists of porous electrodes with a high surface area, anions and cations are attracted and held on the electrodes with opposite charges. The desalinated solution is then expelled from the cell as a product while maintaining a continuous feed flow. In the subsequent step, the electrodes are discharged, releasing the salt from the interfacial double layer region and pores of the electrodes into the bulk liquid phase to create a concentrated solution, which is treated as waste (Kalfa et al., 2020).

In accordance with the desalination process of CDI, the electrode material plays a crucial role in determining CDI's performance. An ideal CDI electrode material should satisfy the following criteria: 1) possessing a significant specific surface area to enhance ion adsorption sites; 2) exhibiting high conductivity and ion mobility; 3) demonstrating outstanding hydrophilicity to guarantee the complete utilization of the electrode's pore structure; 4) maintaining a high level of electrochemical stability under varying pH and voltage conditions to ensure consistent operation and system reliability; 5) being easily molded to meet design specifications (Zhao et al., 2020; Alkhadra et al., 2022; Qin et al., 2019).

There are various materials that have been used in CDI electrodes that meet above conditions, such as carbon-based materials (activated carbon, mesporous carbon, carbon nanotubes, graphene, etc.), pseudocapacitors, or the hybrid of the previous two materials (Luciano et al., 2020; Tan et al., 2020; Sufiani et al., 2020; Torkamanzadeh et al., 2020; Chen et al., 2020; Tian et al., 2020; Zhang et al., 2022; Bharath et al., 2020; Chen et al., 2021). However, carbon is a commonly chosen material for CDI electrodes due to its affordability and superior stability (Cheng et al., 2019). Several carbon-based materials, such as activated carbon, carbon nanotubes (CNTs), and graphene have been employed by researchers as electrode materials. Among these options, activated carbon is favored over graphene and CNTs due to its lower density. The higher density of carbon creates vacant spaces within the electrode, which may potentially be filled by the electrolyte, resulting in increased device weight without any corresponding improvement in capacitance (Kumar et al., 2021; Forouzandeh et al., 2020). Aside of that, the cost-effectiveness and expansive surface area adds the advantage that makes activated carbon emerges as the prominent choice for electrode among various carbonaceous materials (Dubey et al., 2020).

Activated carbon used in CDI electrodes can be fabricated from biowaste, thereby adding its positive value, such as date palm leaflets, lotus leaf, coconut shell, sorghum, etc. (Kyaw et al., 2021; Liu et al., 2020; Adorna Jr et al., 2020; Kim et al., 2021). Among all of the biowaste, the best materials for activated carbon is the one with high lignin content. Lignin contains a higher concentration of carbon atoms compared to the other constituents, making it the most favorable precursor for producing activated carbon (Yang et al., 2020). The lignin content of various common biowastes used as activated carbon precursors is as follows: 40.9% in coconut husk, 22.5% in rice husk, 17% in corn cob, 60.1% in candlenut shell, and 42% in coconut shell (Lebedeva et al., 2022; Rosado et al., 2021; Thangavelu et al., 2018; Klein et al., 2010; Wang and Sarkar, 2018).

Considering the information provided above, opting for materials derived from plants with shells or hard components is the most favorable choice for manufacturing activated carbon, primarily owing to their high lignin content. Thus, those materials are ideal for use in CDI electrodes. In our previous work, we have used sugar palm bunches as a material to obtain activated charcoal with good adsorption capacity and high absorption efficiency (Adrianto et al., 2019; Adrianto et al., 2021). One of the key parameters for commercial realization of CDI is the salt adsorption capacity of the electrodes. While activated carbons are characterized by a high internal surface area and porosity, so it is suitable for CDI electrode. The research on brackish water desalination using CDI which utilizes activated carbon electrodes has been extensively conducted (Samejo et al., 2023; Kyaw et al., 2021; Huynh et al., 2022). Thus, this research focuses on the fabrication of CDI using activated carbon to obtain information regarding the most optimal materials and parameters. In this study, activated carbon electrodes used in CDI are produced from candlenut shells with H_3PO_4 as the activating agent. Parameters observed to achieve optimal carbon performance include material composition, carbonization temperature and duration, type and concentration of activating agent, as well as activation temperature and temperature, which will be further elaborated in the experimental section.

2. EXPERIMENTAL SECTION

2.1 Materials

Capacitive deionization (CDI) is a method used to remove dissolved salts from brackish water or seawater by adsorbing separated ions onto the electrode surfaces. CDI is now a potential method for water desalination (Huang et al., 2017; Gamaethiralalage et al., 2021). In this research, the CDI is made of candlenut shells-based activated carbon as the electrode. Carbon electrodes are more in demand because of the combination of favorable chemical and physical properties, such as high surface area, corrosion resistance, stability to temperature, and high porosity so that it is easy to adsorb ions (Cheng et al., 2019; Dubey et al., 2020).

The raw materials used in this study are candlenut shells gathered from a local farm in South Konawe. The phosporic acid (H_3PO_4) used was produced by Sigma-Adrich and was purchased from CV. Intraco Makassar, polyvinyl alcohol (PVA) was provided by CV. Aloin Labora, alcohol 70% was provided by PT. Likuid Pharmalab Indonesia, while distilled water, Whitman 42 filter paper, and other supporting materials were provided from the local chemical shop.

Table 1. The Mixture Materials of Electrode for Various Thickness

Thickness (mm)	Activated Carbon (g)	PVA (g)	Alcohol (mL)
15	13.5	1.5	22.5
10	9	1	15
8	7.2	0.8	12
6	5.4	0.6	9

2.2 Method

The candlenut shell samples were washed thoroughly with distilled water and then dried under the sunlight. After drying, it was put on a pyrolysis reactor to be carbonized at 400°C for 8 hours. The carbonized candlenut shells are crushed and then sieved with a size of 60, 80, 100, and 200 mesh. After that, each of the sieved carbon sample was activated chemically by H_3PO_4 67% as activation agent with the ratio of 18:25. After that the samples were heated in the furnace at 700°C for 1 hour.

The electrode was prepared from candlenut shell activated carbon. It was made by mixing the activated carbon and PVA with the mass ratio of 9:1 and then dissolved in alcohol. In various thicknesses, there were 4 samples of electrodes as shown in Table 1.

After mixing, the mixture was stirred with a magnetic stirrer at 400 rpm and 70°C heat for 13 minutes. After stirring, the mixture was poured into an aluminum mold with the area of 3 cm × 3 cm with various thicknesses as shown in Table 1. The samples were heated in the oven for 2 hours at 100°C, after that the samples were pressed with a hydraulic jack for 3 tons. The samples were then released from the mold and cooled. The arrangement of the electrode is shown in Figure 1.

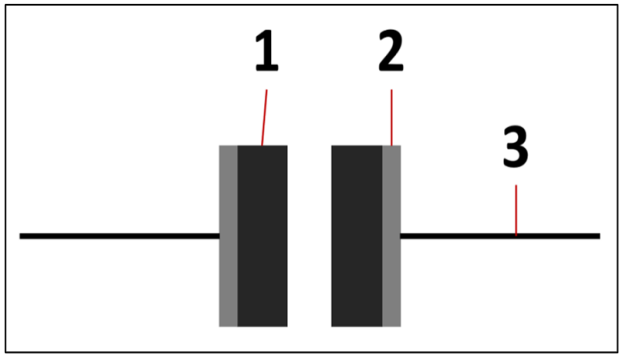

Figure 1. The Arrangement of CDI Electrode: (1) Activated Carbon; (2) Collector (Aluminum); (3) Copper Wire

Sample characterization conducted was the examination of its capacitance. The circuit used was an RC circuit (McLucas and Broomfield, 2010) as shown in Figure 2.

The sample produced is then used as a capacitor in the RC circuit as shown in Figure 2. The capacitor was then connected

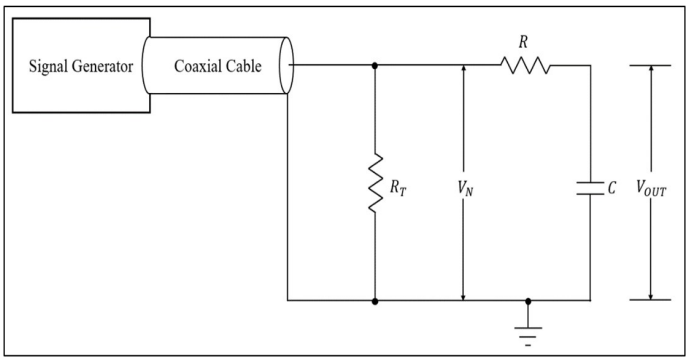

Figure 2. The RC Circuit used for Capacitance Determination

with an $R = 10\,k\Omega$ resistor as a series circuit. The capacitance was calculated with Equation 1,

$$C = \frac{\sqrt{\left(\frac{V_{in}}{V_{out}}\right)^2 - 1}}{2\pi f R} \quad (1)$$

Where C is electrode capacitance, f is the frequency of the signal generator used, and R is the resistance of the resistor.

Desalination was done by letting the seawater flow through the spacer. Seawater salinity was measured with a hand refractometer, while the decrease of salinity was calculated with Equation 2.

$$\Delta S(\%) = \frac{S_0 - S_i}{S_0} \times 100\% \quad (2)$$

where ΔS is the decrease of salinity, S_0 is initial salinity, and S_i is the final salinity of seawater.

3. RESULTS AND DISCUSSION

The first result examined is the effect of the thickness of the activated charcoal electrode from candlenut shells on its capacitance. By varying the electrode thickness by 6 mm, 8 mm, 10 mm, and 15 mm, capacitance values were obtained, and each of them is presented in Figure 3.

Figure 3 shows the capacitance value for electrodes with 6 mm, 8 mm, 10 mm, and 15 mm thickness. It demonstrates that the increase in thickness will decrease the electrode's capacitance. The maximum value obtained is 122.96 nF for a 6 mm electrode. This shows that a thin electrode can reduce the resistance of the candlenut shell-based activated charcoal, thereby providing easier access for ions to penetrate the pores of the electrode. The thinner the electrode, the easier for ions to diffuse so that the resulting capacitance value will be higher. This result is in agreement with the research conducted by Xi et al. (2023). Thicker electrodes decrease the capacitance. Li et al. (2020) stated that thicker electrodes will have longer relaxation time. This will cause a longer time for the ions to

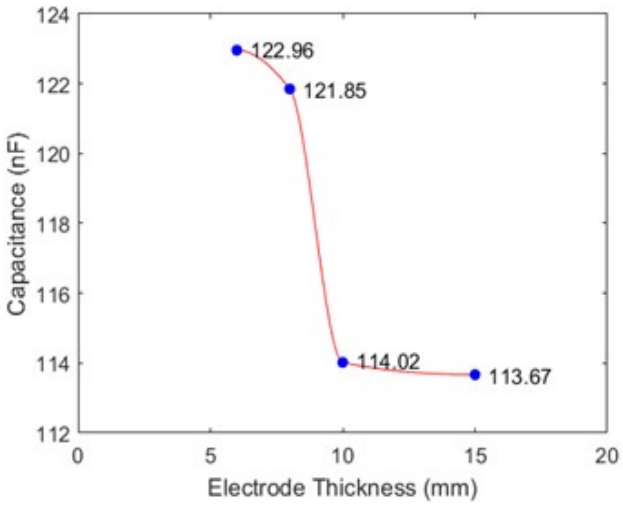

Figure 3. The Effect of Electrode Thickness on its Capacitance

be adsorbed onto the electrode's pores, not all pores can be accessed by ions. The thickness of 6 mm is the optimal value, because the thinner electrodes will be cracked in the pressing process in this study.

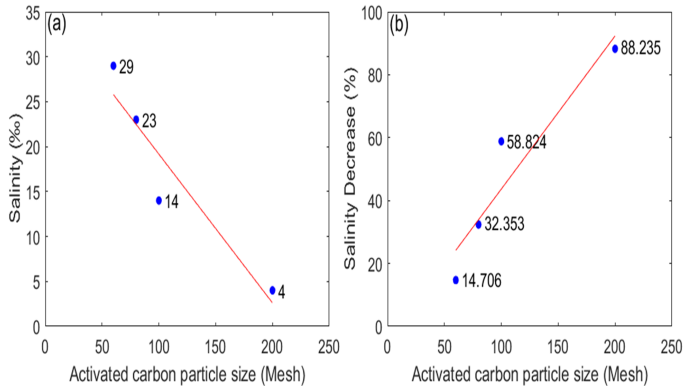

Figure 4. The Effect of Activated Charcoal Particle Size on (a) Salinity (‰) and (b) Salinity Decrease (%)

Figure 4 (a) shows how variation of activated carbon particle size affects seawater salinity value after desalination for 60, 80, 100, and 200 mesh grain sizes. The initial salinity of seawater before desalination is 34‰. The biggest size of the particle, 60 mesh, only decreases the salinity to 29‰ while the smallest particle size, 200 mesh decreases the salinity to 4‰. It means that the decrease in particle size of activated carbon used in CDI electrodes will decrease the salinity. This happened because smaller particles increase capacitance and higher capacitance will increase the desalination performance. It has been shown before that the capacitance of an electrode increase as the particle size decrease (Liu et al., 2018). Furthermore, Wang et al. (2022) stated that the ability of an electrode, especially its capacitance play an important role in desalination performance. Higher capacitance will result in higher salt electrosorption capacity. This will cause the decrease in salinity for desalinated seawater, as shown in Figure 4 (a). Also, Li et al. (2020) explained that the greater the capacitance value, the greater the capacitor's ability to store charge, so if this is applied to the CDI system, the greater the capacitance value of the carbon electrode, the greater the capability of the CDI system.

Figure 4 (b) exhibits how the decrease of salinity is affected by the size of activated carbon particle size. As could be seen in Equation 2, the decrease in salinity is also affected by the difference in initial and final salinity (that is, the seawater salinity before and after desalination). The higher the difference, the higher the decrease in salinity. The biggest particle size, 60 mesh, has the smallest decrease, that is 14.70%, while the smallest particle size, 200 mesh, has bigger decrease in salinity, 88.23%.

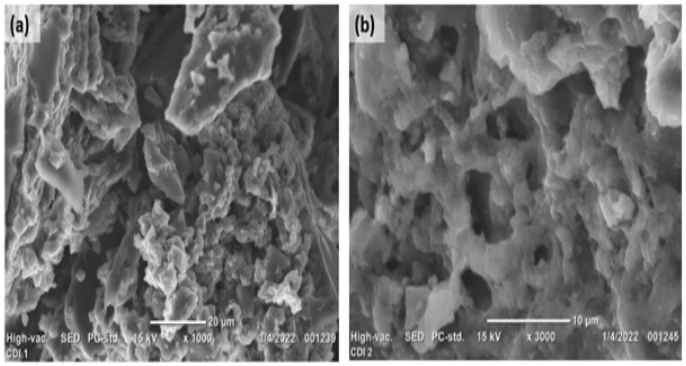

Figure 5. The SEM Imaging of 200 Mesh Activated Carbon Electrode Surface (a) Before, and (b) After the Desalination Process

Figure 5 shows the SEM imaging of the candlenut shell-based activated carbon electrode surface used in CDI. The sample shown is for 200 mesh particle size. It is shown that before the desalination process, the surface has coarse grain and many pores. After the desalination process, the electrode has a finer surface. It happens because the pores of the electrode already adsorb the ions from deionized salt in seawater. These results are consistent with the findings of research conducted by Kushwaha et al. (2020), illustrating that salt ions adsorbed onto the surface of a carbon electrode occupy the electrode pores, leading to a change in the surface from initially porous to a finer texture. Li et al. (2021) also presented similar results, suggesting that the electrode surface becomes finer after the adsorption of salt ions. Additionally, Jiang et al. (2020) mentioned that, in the course of the desalination process, salt ions get adsorbed onto the electrode surface, forming an electrical double layer on the inner surface of the electrode. This adds proof of the effectiveness of finer particles as material for electrodes in CDI for seawater desalination.

To determine the functional groups which present in the

Table 2. Characteristic FTIR Peaks of Electrode Sample Before and After Desalination

Functional Group	Observed Wavenumber (cm^{-1})		
	Before	After (+)	After (-)
O−H	3466.08	3446.79	3456.44
O=C=O	2366.66	2360.87	2364.73
C=C	1637.56	1570.06	1656.85
	962.48	-	-
C−O	1240.23	1228.66	-
	1159.22	1126.43	1070.49
M−N & M−O	684.73	-	667.37
	570.93	-	613.36
	505.35	-	572.86

CDI electrode, characterization was conducted using FTIR (Fourier Transform Infrared). Figure 6 and Table 2 show the result of FTIR characterization on the electrode before and after the desalination process.

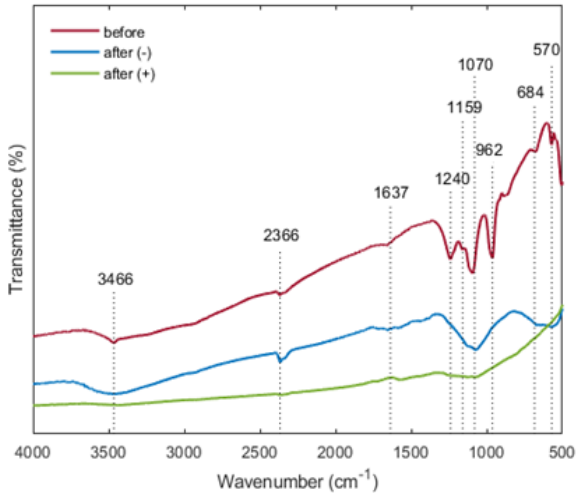

Figure 6. The FTIR Spectrum of Electrode Sample Before and After Desalination. After (-) Represents the Negative Electrode After Desalination, After (+) Represents the Positive Electrode After Desalination

Figure 6 shows the FTIR spectrum for the activated carbon electrode sample before (represented by "before") and after desalination (represented by "after (+)" for the positive electrode and "after (-)" for the negative electrode). The spectrum of "before" sample showed more peaks than the spectrum for the "after (+)" and "after (-)" samples. In general, the three samples have similar functional groups. In Table 2, the peak transmission wavenumbers are showed in detail. The peak numbers 3466.08 cm^{-1} (before), 3446.79 cm^{-1} (after (+)), and 3456.44 cm^{-1} (after (-)) refer to OH stretching bonds which indicate the existence of the OH hydroxyl functional group. The sharp peak at 3466.08 cm^{-1} that emerges in the broad OH band in the "before" sample indicates the characteristic of activated carbon by H_3PO_4, as demonstrated by Mohtashami et al. (2018). The carbon dioxide (O=C=O) is also present in the sample at 2366.66 cm^{-1} (before), 2360.87 cm^{-1} (after (+)), and 2364.73 cm^{-1} (after (-)). It is shown that carbon oxidation also happened at the electrode. In the negative electrode, it could be seen that the carbon dioxide peak is stronger than desalination. In the positive electrode, it may not solely electrochemically store anions but could also actively participate in the oxidation process, with the carbon electrode initially incorporating oxygen-containing groups and, potentially, eventually being partially converted into CO_2. This results in a reduction in carbon mass and a deterioration in CDI performance (Zhang et al., 2018). The results also showed the presence of alkene C=C stretching in all of the samples at 1637.56 cm^{-1} (before), 1570.06 cm^{-1} (after (+)), and 1656.85 cm^{-1} (after (-)). The peak is not strong with broad characteristics. The distinctive difference is demonstrated at the wavenumber range from 900 – 1300 cm^{-1}. In this range, there are several sharp peaks in the "before" sample at 962.48 cm^{-1} due to the existence of alkene C=C bending and 1159.22 cm^{-1} and also 1240.23 cm^{-1} due to the C−O stretching. In the same range, the "after (-)" sample of the negative electrode did not exhibit a sharp peak, but a broad one that peaked at 1070.49 cm^{-1} as C−O stretching is also present. In contrast with the negative electrode, the "after (+)" sample of the positive electrode did not exhibit a sharp or broad peak, but only an almost negligible one at 1126.43 cm^{-1}. This indicates that the positive electrode has adsorbed the anion from deionized brackish water. After a long time, the accumulation of anion results in carbon oxidation that results in CDI electrode degradation (Zhang et al., 2018). Aside from that, the peaks at low intensity bands in the region of about 500 – 600 cm^{-1} are attributed to the presence of metal oxide and metal nitride vibration (Köse and Necefoğlu, 2008). Several peaks in the "before" sample were detected at 684.73 cm^{-1}, 570.93 cm^{-1}, and 505.35 cm^{-1}. The "after (-)" exhibit a broad peak with a maximum value of 667.37 cm^{-1}, 613.36 cm^{-1}, and 572.86 cm^{-1}. Unlike the "before" and "after (+)" sample, the "after (-)" sample did not show any peaks at this region.

4. CONCLUSION

Based on the work done in this study, it is concluded that optimum CDI should have higher capacitance. It could be obtained with the thinner electrode, that is 6 mm which produces the highest capacitance, 122.96 nF. For the desalination of seawater, it is shown that the smallest/finest particle size will result in the best desalination performance, where 200 mesh particle size will result in the decrease of salinity from 34‰ to 4‰. That is 88.23% decrease of salinity. Therefore, the using of candlenut shell-based activated carbon as the electrode in CDI is proven to be able to obtain good performance for seawater desalination.

5. ACKNOWLEDGEMENT

The authors are grateful to LPPM Universitas Halu Oleo for their financial support in aiding this research by DIPA funding for research in 2022.

REFERENCES

Adorna Jr, J., M. Borines, and R. A. Doong (2020). Coconut Shell Derived Activated Biochar–Manganese Dioxide Nanocomposites for High Performance Capacitive Deionization. *Desalination*, **492**; 114602

Adrianto, N., V. Mongkito, S. Fayanto, M. Anas, and R. Eso (2019). Characterization of Activated Charcoal from Sugar Palm Bunches (*Arengga pinnata* (Wurmb) Merr) and the Application As Adsorbent Lead (Pb), Copper (Cu) and Chrome (Cr) in Solution. In *Journal of Physics: Conference Series*, volume 1321. IOP Publishing, page 022002

Adrianto, N., A. M. Panre, R. M. Tumbelaka, and M. Anas (2021). The Microwave Activation Effect on the Surface Morphology of Activated Charcoal from *Arenga pinnata* Merr Bunches. In *AIP Conference Proceedings*, volume 2338. AIP Publishing

Alkhadra, M. A., X. Su, M. E. Suss, H. Tian, E. N. Guyes, A. N. Shocron, K. M. Conforti, J. P. De Souza, N. Kim, and M. Tedesco (2022). Electrochemical Methods for Water Purification, Ion Separations, and Energy Conversion. *Chemical Reviews*, **122**(16); 13547–13635

Bharath, G., A. Hai, K. Rambabu, D. Savariraj, Y. Ibrahim, and F. Banat (2020). The Fabrication of Activated Carbon and Metal-Carbide 2D Framework-Based Asymmetric Electrodes for the Capacitive Deionization of Cr(VI) Ions toward Industrial Wastewater Remediation. *Environmental Science: Water Research & Technology*, **6**(2); 351–361

Chen, B., A. Feng, R. Deng, K. Liu, Y. Yu, and L. Song (2020). MXene As a Cation-Selective Cathode Material for Asymmetric Capacitive Deionization. *ACS Applied Materials & Interfaces*, **12**(12); 13750–13758

Chen, Z., X. Xu, Z. Ding, K. Wang, X. Sun, T. Lu, M. Konarova, M. Eguchi, J. G. Shapter, L. Pan, et al. (2021). Ti_3C_2 Mxenes-Derived $NaTi_2(PO_4)_3$/MXene Nanohybrid for Fast and Efficient Hybrid Capacitive Deionization Performance. *Chemical Engineering Journal*, **407**; 127148

Cheng, Y., Z. Hao, C. Hao, Y. Deng, X. Li, K. Li, and Y. Zhao (2019). A Review of Modification of Carbon Electrode Material in Capacitive Deionization. *RSC Advances*, **9**(42); 24401–24419

Dubey, P., V. Shrivastav, P. H. Maheshwari, and S. Sundriyal (2020). Recent Advances in Biomass Derived Activated Carbon Electrodes for Hybrid Electrochemical Capacitor Applications: Challenges and Opportunities. *Carbon*, **170**; 1–29

Forouzandeh, P., V. Kumaravel, and S. C. Pillai (2020). Electrode Materials for Supercapacitors: A Review of Recent Advances. *Catalysts*, **10**(9); 969

Gamaethiralalage, J., K. Singh, S. Sahin, J. Yoon, M. Elimelech, M. Suss, P. Liang, P. Biesheuvel, R. L. Zornitta, and L. De Smet (2021). Recent Advances in Ion Selectivity with Capacitive Deionization. *Energy & Environmental Science*, **14**(3); 1095–1120

Gong, S., H. Wang, Z. Zhu, Q. Bai, and C. Wang (2019). Comprehensive Utilization of Seawater in China: A Description of the Present Situation, Restrictive Factors and Potential Countermeasures. *Water*, **11**(2); 397

He, C., Z. Liu, J. Wu, X. Pan, Z. Fang, J. Li, and B. A. Bryan (2021). Future Global Urban Water Scarcity and Potential Solutions. *Nature Communications*, **12**(1); 4667

Huang, Z. H., Z. Yang, F. Kang, and M. Inagaki (2017). Carbon Electrodes for Capacitive Deionization. *Journal of Materials Chemistry A*, **5**(2); 470–496

Huynh, L. T. N., T. N. Tran, T. T. N. Ho, X. H. Le, V. H. Le, and T. H. Nguyen (2022). Enhanced Electrosorption of NaCl and Nickel (II) in Capacitive Deionization by CO_2 Activation Coconut-Shell Activated Carbon. *Carbon Letters*, **32**(6); 1531–1540

Jiang, Y., S. I. Alhassan, D. Wei, and H. Wang (2020). A Review of Battery Materials As CDI Electrodes for Desalination. *Water*, **12**(11); 3030

Kalfa, A., B. Shapira, A. Shopin, I. Cohen, E. Avraham, and D. Aurbach (2020). Capacitive Deionization for Wastewater Treatment: Opportunities and Challenges. *Chemosphere*, **241**; 125003

Kim, M., H. Lim, X. Xu, M. S. A. Hossain, J. Na, N. N. Awaludin, J. Shah, L. K. Shrestha, K. Ariga, and A. K. Nanjundan (2021). Sorghum Biomass-Derived Porous Carbon Electrodes for Capacitive Deionization and Energy Storage. *Microporous and Mesoporous Materials*, **312**; 110757

Klein, A. P., E. S. Beach, J. W. Emerson, and J. B. Zimmerman (2010). Accelerated Solvent Extraction of Lignin from *Aleurites moluccana* (Candlenut) Nutshells. *Journal of Agricultural and Food Chemistry*, **58**(18); 10045–10048

Köse, D. and H. Necefoğlu (2008). Synthesis and Characterization of *bis*(Nicotinamide) *m*-Hydroxybenzoate Complexes of Co (II), Ni (II), Cu (II) and Zn (II). *Journal of Thermal Analysis and Calorimetry*, **93**; 509–514

Kumar, S., G. Saeed, L. Zhu, K. N. Hui, N. H. Kim, and J. H. Lee (2021). 0D to 3D Carbon-Based Networks Combined with Pseudocapacitive Electrode Material for High Energy Density Supercapacitor: A Review. *Chemical Engineering Journal*, **403**; 126352

Kushwaha, R., D. Bhaskar, Sonam, and D. Mohan (2020). An Experimental Study on Some Parameters for Defluoridation Using Capacitive Deionization with Carbon Electrodes. *Journal of the Indian Chemical Society*, **97**(3); 368–372

Kyaw, H. H., S. M. Al-Mashaikhi, M. T. Z. Myint, S. Al-Harthi, E.-S. I. El-Shafey, and M. Al-Abri (2021). Activated Carbon Derived from the Date Palm Leaflets As Multifunctional Electrodes in Capacitive Deionization System. *Chemical Engineering and Processing-Process Intensification*, **161**; 108311

Lebedeva, D., S. Hijmans, A. P. Mathew, E. Subbotina, and

J. S. Samec (2022). Waste-to-Fuel Approach: Valorization of Lignin from Coconut Coir Pith. *ACS Agricultural Science & Technology*, **2**(2); 349–358

Li, L., C. Wang, K. Feng, D. Huang, K. Wang, Y. Li, and F. Jiang (2021). Kesterite Cu_2ZnSn_4 Thin-Film Solar Water-Splitting Photovoltaics for Solar Seawater Desalination. *Cell Reports Physical Science*, **2**(6); 100468

Li, Z., S. Gadipelli, H. Li, C. A. Howard, D. J. Brett, P. R. Shearing, Z. Guo, I. P. Parkin, and F. Li (2020). Tuning the Interlayer Spacing of Graphene Laminate Films for Efficient Pore Utilization Towards Compact Capacitive Energy Storage. *Nature Energy*, **5**(2); 160–168

Lin, S., H. Zhao, L. Zhu, T. He, S. Chen, C. Gao, and L. Zhang (2021). Seawater Desalination Technology and Engineering in China: A Review. *Desalination*, **498**; 114728

Liu, G., L. Qiu, H. Deng, J. Wang, L. Yao, and L. Deng (2020). Ultrahigh Surface Area Carbon Nanosheets Derived from Lotus Leaf with Super Capacities for Capacitive Deionization and Dye Adsorption. *Applied Surface Science*, **524**; 146485

Liu, J., J. Wang, C. Xu, H. Jiang, C. Li, L. Zhang, J. Lin, and Z. X. Shen (2018). Advanced Energy Storage Devices: Basic Principles, Analytical Methods, and Rational Materials Design. *Advanced Science*, **5**(1); 1700322

Luciano, M. A., H. Ribeiro, G. E. Bruch, and G. G. Silva (2020). Efficiency of Capacitive Deionization Using Carbon Materials Based Electrodes for Water Desalination. *Journal of Electroanalytical Chemistry*, **859**; 113840

McLucas, J. and C. Broomfield (2010). Circuit Measures Capacitance or Inductance

Mohammadi, F., M. Sahraei-Ardakani, Y. Al-Abdullah, and G. T. Heydt (2020). Cost-Benefit Analysis of Desalination: A Power Market Opportunity. *Electric Power Components and Systems*, **48**(11); 1091–1101

Mohtashami, S.-A., N. A. Kolur, T. Kaghazchi, R. Asadi-Kesheh, and M. Soleimani (2018). Optimization of Sugarcane Bagasse Activation to Achieve Adsorbent with High Affinity Towards Phenol. *Turkish Journal of Chemistry*, **42**(6); 1720–1735

Naseer, M. N., A. A. Zaidi, H. Khan, S. Kumar, M. T. B. Owais, Y. A. Wahab, K. Dutta, J. Jaafar, M. Uzair, and M. R. Johan (2022). Desalination Technology for Energy-Efficient and Low-Cost Water Production: A Bibliometric Analysis. *Green Processing and Synthesis*, **11**(1); 306–315

Qin, M., A. Deshmukh, R. Epsztein, S. K. Patel, O. M. Owoseni, W. S. Walker, and M. Elimelech (2019). Comparison of Energy Consumption in Desalination by Capacitive Deionization and Reverse Osmosis. *Desalination*, **455**; 100–114

Rosado, M. J., J. Rencoret, G. Marques, A. Gutiérrez, and J. C. Del Río (2021). Structural Characteristics of the Guaiacyl-Rich Lignins from Rice (*Oryza sativa L.*) Husks and Straw. *Frontiers in Plant Science*, **12**; 640475

Samejo, B. A., N. Q. Abro, N. Memon, S. Poddar, and A. Habib (2023). Waste-Derived Stable Carbon Electrodes for Capacitive Deionization Using Poly (Vinyl Alcohol)-Glutaraldehyde As Binder. *Biomass Conversion and Biorefinery*; 1–14

Sufiani, O., H. Tanaka, K. Teshima, R. L. Machunda, and Y. A. Jande (2020). Enhanced Electrosorption Capacity of Activated Carbon Electrodes for Deionized Water Production through Capacitive Deionization. *Separation and Purification Technology*, **247**; 116998

Tan, G., S. Lu, N. Xu, D. Gao, and X. Zhu (2020). Pseudocapacitive Behaviors of Polypyrrole Grafted Activated Carbon and MnO_2 Electrodes to Enable Fast and Efficient Membrane-Free Capacitive Deionization. *Environmental Science & Technology*, **54**(9); 5843–5852

Thangavelu, K., R. Desikan, O. P. Taran, and S. Uthandi (2018). Delignification of Corncob Via Combined Hydrodynamic Cavitation and Enzymatic Pretreatment: Process Optimization by Response Surface Methodology. *Biotechnology for Biofuels*, **11**(1); 1–13

Tian, S., X. Zhang, and Z. Zhang (2020). Capacitive Deionization with MoS_2/g-C_3N_4 Electrodes. *Desalination*, **479**; 114348

Torkamanzadeh, M., L. Wang, Y. Zhang, O. Budak, P. Srimuk, and V. Presser (2020). MXene/activated-Carbon Hybrid Capacitive Deionization for Permselective Ion Removal at Low and High Salinity. *ACS Applied Materials & Interfaces*, **12**(23); 26013–26025

Wang, Q. and J. Sarkar (2018). Pyrolysis Behaviors of Waste Coconut Shell and Husk Biomasses. *Towards Energy Sustainability*, **3**(1); 34–43

Wang, W., K. Li, G. Song, M. Zhou, and P. Tan (2022). Activated Carbon Aerogel as an Electrode with High Specific Capacitance for Capacitive Deionization. *Processes*, **10**(12); 2330

Xi, W., Y. Zhang, R. Wang, Y. Gong, B. He, H. Wang, J. Guo, F. Jiao, and J. Jin (2023). The Effect of Electrode Thickness and Electrode/electrolyte Interface on the Capacitive Deionization Behavior of the $Ti_3C_2T_x$ Mxene Electrodes. *Journal of Alloys and Compounds*, **947**; 169701

Xing, W., J. Liang, W. Tang, D. He, M. Yan, X. Wang, Y. Luo, N. Tang, and M. Huang (2020). Versatile Applications of Capacitive Deionization (CDI)-based Technologies. *Desalination*, **482**; 114390

Yang, Z., R. Gleisner, D. H. Mann, J. Xu, J. Jiang, and J. Zhu (2020). Lignin Based Activated Carbon Using H_3PO_4 Activation. *Polymers*, **12**(12); 2829

Zapata-Sierra, A., M. Cascajares, A. Alcayde, and F. Manzano-Agugliaro (2021). Worldwide Research Trends on Desalination. *Desalination*, **519**; 115305

Zhang, B., A. Boretti, and S. Castelletto (2022). Mxene Pseudocapacitive Electrode Material for Capacitive Deionization. *Chemical Engineering Journal*, **435**; 134959

Zhang, C., D. He, J. Ma, W. Tang, and T. D. Waite (2018). Faradaic Reactions in Capacitive Deionization (CDI)-problems and Possibilities: A Review. *Water Research*, **128**; 314–330

Zhao, X., H. Wei, H. Zhao, Y. Wang, and N. Tang (2020). Electrode Materials for Capacitive Deionization: A Review. *Journal of Electroanalytical Chemistry*, **873**; 114416

